Article

Not peer-reviewed version

Life Cycle Assessment of Fluoride Removal from Mining Effluents Using Electrocoagulation and Biogenic CO_2

Elbert Muller Nigri , André Luiz Alvarenga Santos , Sonia D. F. Rocha *

Posted Date: 16 September 2025

doi: 10.20944/preprints202509.1426.v1

Keywords: ReCiPe Endpoint; pH regulator; energy cogeneration; mineral wastewater; CO2 capture; electrocoagulation

Article

Life Cycle Assessment of Fluoride Removal from Mining Effluents Using Electrocoagulation and Biogenic CO_2

Elbert Nigri [1], André Santos [2] and Sônia Rocha [3,*]

[1] SENAI Innovation and Technology Center, (CIT-SENAI), Belo Horizonte, Brazil
[2] Center for Mineral Technology (CETEM), Rio de Janeiro, Brazil
[3] Department of Mining Engineering, Universidade Federal de Minas Gerais (UFMG), Belo Horizonte, Brazil
* Correspondence: sdrocha@demin.ufmg.br

Abstract

Fluoride-containing wastewater poses a significant environmental challenge, especially in the mineral processing sector. This study applies a life cycle assessment (LCA) to evaluate an electrocoagulation-based treatment process, integrating biogas-derived CO_2 for pH regulation and cogeneration of electricity, using the Egalitarian perspective, which is the most precautionary that takes into account the longest time-frame and impact types that are not yet fully established but for which some indication is available. The LCA considered five subsystems: electrocoagulation, pH adjustment, sedimentation, pumping, and sludge transport, across three operational scenarios. Scenario 1 (S1) employed hydrochloric acid for pH control, Scenario 2 (S2) used biogas exclusively for pH regulation, and Scenario 3 (S3) combined biogas-based pH adjustment with power generation. Results showed an environmental impact ranking of S3 < S1 < S2, with S3 reducing overall impacts from 12.5 Pt to 6.4 Pt compared to S1. The electrocoagulation unit was the dominant contributor to environmental burdens; however, in S3, the pH adjustment subsystem delivered a net environmental benefit through surplus electricity generation. Additionally, sludge reuse as a raw material for brick production, implemented in all scenarios, further mitigated impacts. Human health emerged as the most affected endpoint, driven mainly by toxicity (carcinogenic and non-carcinogenic), climate change potential, marine ecotoxicity, and particulate matter formation. These findings highlight the benefits of integrating biogas utilization and sludge valorization into industrial wastewater management strategies.

Keywords: ReCiPe Endpoint; pH regulator; energy cogeneration; mineral wastewater; CO_2 capture; electrocoagulation

1. Introduction

Industrial fluoride-containing wastewater significantly contributes to the pollution of groundwater, surface water bodies, and soil, with substantial adverse environmental impacts [1,2]. Fluoride concentrations in industrial effluents are often substantially higher than in natural waters, ranging from 10 to 6,500 $mg \cdot L^{-1}$ [3–7]. These effluents typically originate from the production of niobium(hydrofluoric acid is used as activator in flotation) and phosphates (fluorapatite bearing) ores processing, aluminum fluoride, semiconductors, fertilizers, glass industries and from the production of high-strength and superconducting metal alloys [8,9]. Chronic exposure to fluoride concentrations above 2 $mg \cdot L^{-1}$ can lead to dental fluorosis and, in severe cases, skeletal fluorosis, osteoporosis, arthritis, male infertility, Alzheimer's disease, and damage to the liver, kidneys, or parathyroid gland [10–12].

The impact of fluoride in human health is well known [1–13]. Under chronic fluoride exposure at 100 ppm, the highest accumulation was observed in the liver, followed by the kidneys and heart.

Preprints.org (www.preprints.org) | NOT PEER-REVIEWED | Posted: 16 September 2025 doi:10.20944/preprints202509.1426.v1

This distribution was associated with significant biochemical alterations, including elevated plasma levels of dehydrogenase, aminotransferases, kidney injury molecule-1 (KIM-1), and other renal biomarkers, together with a reduction in total plasma proteins and albumin. The findings demonstrate that fluoride accumulation exerts concentration-dependent hepatotoxic, nephrotoxic, and cardiotoxic effects, underscoring the substantial health risks posed by chronic fluoride intake in endemic areas [13].

Various technologies have been applied to adjust fluoride concentrations to acceptable levels for discharge or human consumption [14]. From them, electrocoagulation (EC) has proved to be particularly effective for both drinking water and industrial wastewater treatment [15–23]. EC offers several advantages such as simple and compact design, ease of automation, no need for chemical additives, quick operation, and minimal sludge production [24,25]. However, pH control is a critical factor in EC-based fluoride removal. This is because effective formation of $Al(OH)_3$, a key agent in the process, depends on pH and is favored in the pH range of 6–8 [7,26]. This commands the use of pH regulators to maintain the optimal pH range during the treatment.

From another side, CO_2 capture systems from flue gases and other systems have a potential effect on reducing impacts on climate change. Various technologies have been developed to capture CO_2 from flue gases and other sources, each one with distinct advantages and limitations. These technologies include absorption, adsorption, membrane separation, cryogenic distillation, and electrochemical processes [27]. The effectiveness of these systems in reducing emissions and their potential to mitigate climate change varies based on their application, cost, and efficiency. In this paper, it is addressed the use of CO_2 for pH control, as an alternative to traditional acids such as HCl or H_2SO_4, avoiding introducing chloride or sulfate ions into the treated water and contributing to reduce CO_2 emissions. Control of pH is crucial for enhancing CO_2 absorption in water, as it facilitates the conversion of CO_2 into bicarbonate (HCO_3^-). Absorption must be carried out at optimal pH to get maximum efficiency. This method may be particularly beneficial for smaller plants that emit limited amounts of CO_2, as it does not require extensive transport and storage infrastructure [28]. Considering the high content of CO_2 in biogas (35-40% in vol), and the need to separate it from methane (55-60% in vol) [w], integrating biogas into the treatment process, can contribute to reducing greenhouse gas emissions and reduce the CO_2 impact on environment. In a previous work, the separation of CO_2 from biogas produced in anaerobic biodigesters allowed its separation from methane, enhancing its use for energy generation [29].

Evaluation of the environmental performance of fluoride treatment processes may be done by Life Cycle Assessment (LCA) tools [33,34]. providing a comprehensive assessment of environmental burdens, related to material and energy inputs. This has been widely applied to assess and compare wastewater treatment technologies [34,36–39]. LCA methodologies have also evolved to access associated toxicity impacts on human health and ecosystems [34,40]. Despite many studies on fluoride removal by electrocoagulation [15–26], LCA applied specifically to the fluoride electrocoagulation (EC) are scarce. The environmental performance comparing two technologies for removing arsenic (As^{3+}) and fluoride (F^-) from groundwater is presented in literature [41]. They used the GaBi software with midpoint methods (CML 2001 and TRACI) and report that, compared to adsorption, EC is identified as a more sustainable and cost-effective option for community-level groundwater treatment.

On the other hand, LCA also accounts for indirect environmental impacts, such as those related to the production of fuels and energy used in effluent treatment processes [36]. Using renewable energy to power EC systems can mitigate concerns related to greenhouse gas emissions associated with fossil-based electricity [42,43]. The electrocoagulation (EC) process produces sludge with significant potential for resource recovery and environmental sustainability. The valorization of EC-generated sludge offers potential for waste minimization and further impact reduction [44]. Potential applications of this sludge containing fluorides can be cited, as in construction materials [45,46)], as adsorbents [47–49], and as active corrosion inhibitors for aluminum [50]. Nevertheless, challenges

 doi:10.20944/preprints202509.1426.v1

related to energy consumption and electrode stability remain and must be addressed to optimize the process for widespread use.

In the context of fluoride-containing wastewater treatment by electrocoagulation, where strict pH control is required and reducing CO_2 emissions is a priority, this study applies the LCA methodology to evaluate the environmental impacts of different pH control strategies in a full-scale electrocoagulation plant. The three strategies considered are: (i) pH adjustment using hydrochloric acid (HCl), (ii) pH regulation with biogenic CO_2 derived from biodigester-sourced biogas, and (iii) combined use of biogenic CO_2 for pH regulation together with methane-enriched biogas for electricity generation

Description of system and conditions

2.1. LCA methodology

The LCA methodology defined by the ISO 14040:2006 series [35,51] was applied in this study. LCA modeling and impact estimation were performed using SimaPro® 9.1. This software was selected because it provides access to multiple databases and impact assessment methods, along with a robust graphical interface that facilitates the identification of the processes with the greatest impacts [52]. The ReCiPe 2016 v1.1 endpoint method was applied to estimate the environmental impacts of wastewater treatment. The Egalitarian (E) perspective was selected, as it is the most precautionary approach, accounting for the longest time horizon and including impact categories that are not yet fully established, but for which preliminary evidence exists [53,54]. ReCiPe allows choosing to use midpoint indicators or endpoint indicators. Each method has been created from three different perspectives.

The endpoint method deals with human health, natural resources and the environment and offers long-term environmental impacts associated with uncertainty compared to the midpoint analysis. The global environmental impact is the weighted sum of endpoint damages to human health, ecosystems, and resources, providing a single overall indicator of environmental burden [55].

2.2. Goal and scope of the study

The functional unit for the electrocoagulation process was defined as 1 m^3 of treated effluent [56], with a final fluoride concentration of less than 10 ppm. The process was divided into 5 subsystems (Figure 1): electrocoagulation unit, pH control unit, sedimentation unit, pumping, and waste transport.

 doi:10.20944/preprints202509.1426.v1

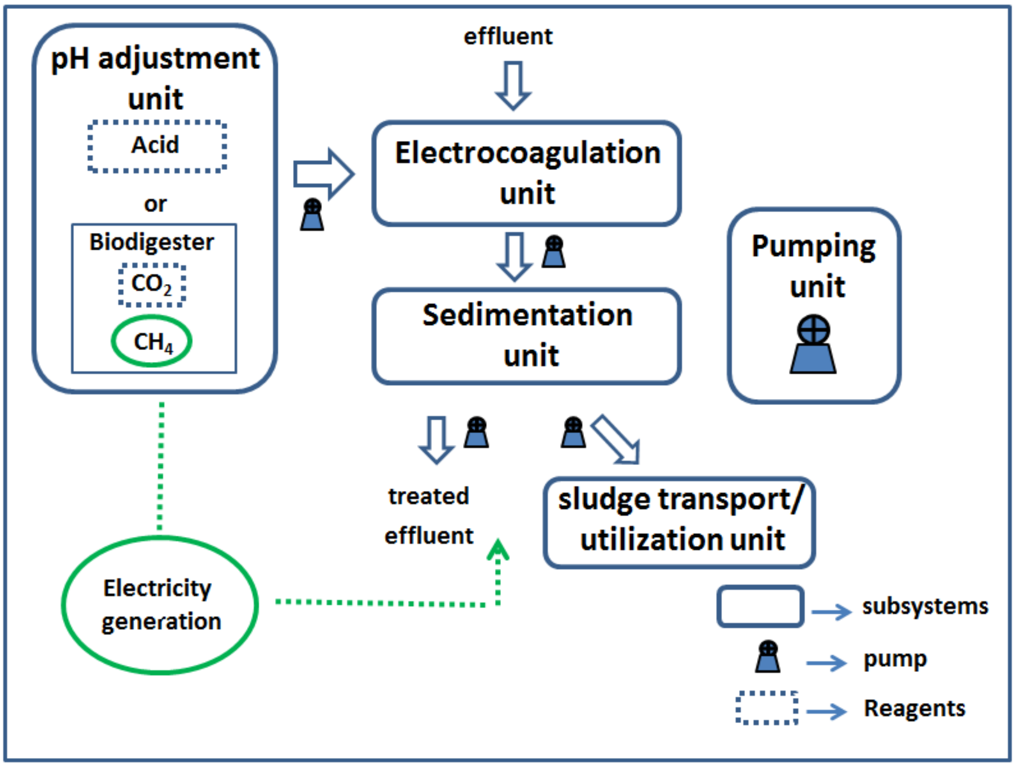

Figure 1. System and subsystems units applied to this study.

Three different scenarios (Table 1) were evaluated. In scenario S1 HCl was used to control the pH while in scenarios S2 and S3, CO_2 biogas was applied. Additionally, in scenario S3, after pH control the residual gas was used to produce electrical energy. The generated energy was reused in the system. The "Gate-to-Gate" methodology was considered, that is, starting with the collection of effluent and ending with its discharge.

Table 1. Scenarios description**.**

Scenario	Reagent	Function
S1	HCl	pH control
S2	CO_2 from biogas	pH control
S3	CO_2 from biogas	pH control and energy source
In scenarios S1, S2 and S3, the generated sludge was used to manufacture building bricks.		

2.3 Life Cycle inventory (LCI)

Experiments were carried out on a lab scale according to schematic setup shown in Figure 2. The biodigester used in this study (Homebiogas) was fed with 5kg of corn straw, able to produce about 700L of biogas per week. The biogas (50.1% CO_2, 47.9% CH_4, 0.8% O2, 40ppm CO, and 7ppm H_2S) was analyzed by a gas analyzer Landtec GEM5000. For comparative purposes, experiments were also carried out using acid for pH control.

Energy spent, wear of aluminum plates, volume of gas or acid, residual fluoride concentration, among others, were collected from experiments and computed as a function of the volume of treated effluent. More information can be found on [30].

Preprints.org (www.preprints.org) | NOT PEER-REVIEWED | Posted: 16 September 2025 doi:10.20944/preprints202509.1426.v1

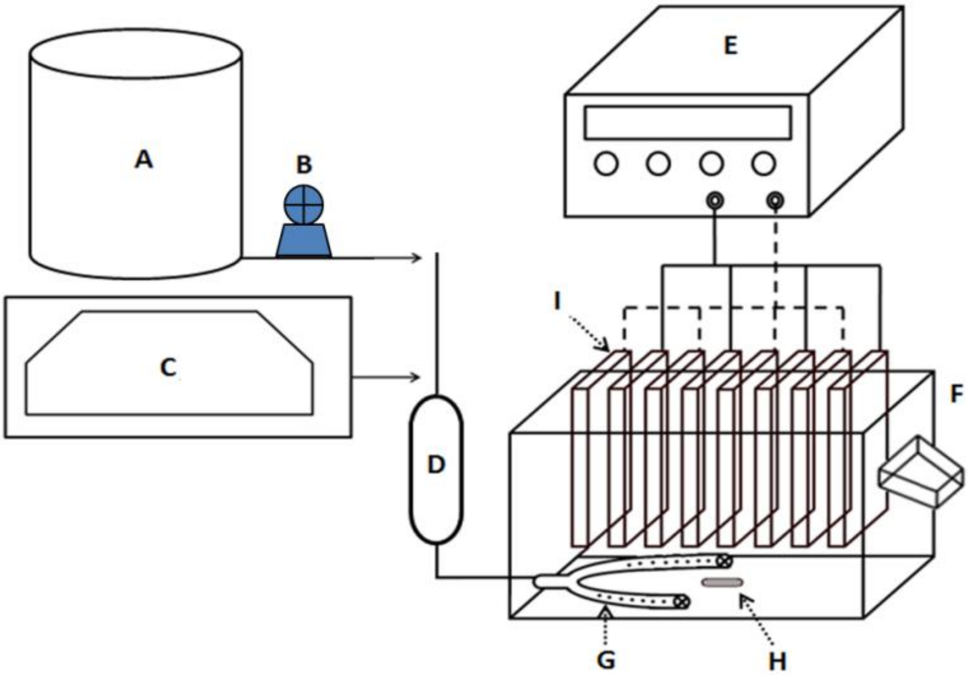

Figure 2. Experimental setup: A - wastewater storage; B - peristaltic pump; C - biodigester or acid; D - gas and wastewater mixer; E - DC power supply; F - electrochemical cell; G - gas/wastewater sprinkler; H - magnetic stirrer; I - aluminum electrodes.

From experimental and literature data [30] an electrocoagulation unit of 23 m^3/day was designed, as well as the measurement of pumping energy expenditure [57]. The unit shown in Figure 3 also includes solid-liquid separation by sedimentation.

The sludge generated in the process is stored in a stockpile, collected and transported to a brick factory. The inputs used in the structural part of the project, as well as the spending during use, such as aluminum, energy and reagents, are shown in tables 2 – 6, divided into subsystems as described in item 2.2.

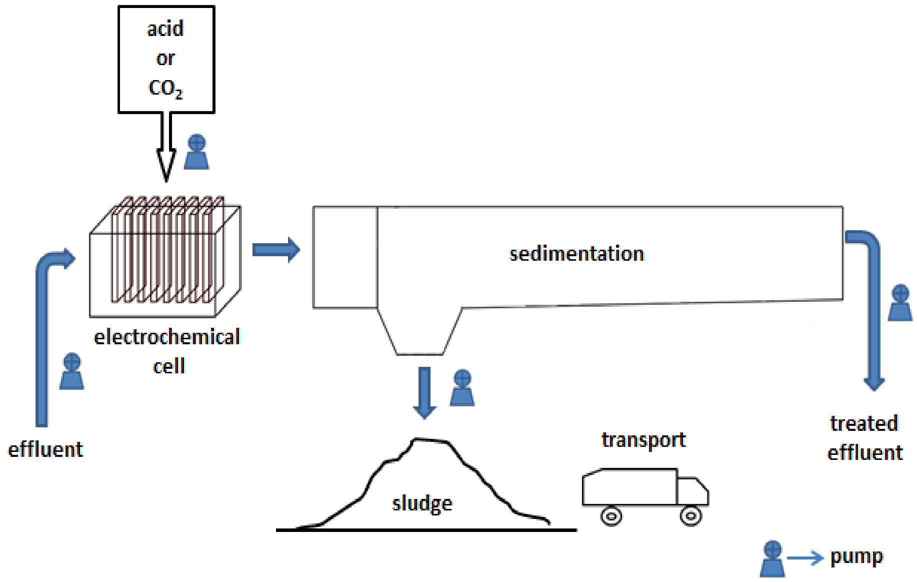

Figure 3. Schematic of the electrocoagulation treatment plant for fluoride removal.

Preprints.org (www.preprints.org) | NOT PEER-REVIEWED | Posted: 16 September 2025 doi:10.20944/preprints202509.1426.v1

A real stream from mining industry with the characteristics shown in **Table 2** was used in this study. According to the Brazilian guidelines [58] the residual fluoride in a treated effluent cannot exceed 10mg.L^{-1}. After treatment, the effluent presented 7.9-10.3 mg.L^{-1} of fluoride with a pH of 6.5-7.1 thus complying with the regulation [30].

Table 2. Chemical characterization of the wastewater [30].

Parameter	Value
pH	7.8
Conductivity (µS.cm^{-1})	6056.0
Fluoride (mg.L^{-1})	134.0
Calcium (mg.L^{-1})	4.4
Sodium (mg.L^{-1})	632.0
Aluminum (mg.L^{-1})	<5.0*
Chloride (mg.L^{-1})	1424.0
Sulfate (mg.L^{-1})	69.0
Alkalinity carbonates and hydroxides (mg.L^{-1})	0.0
Alkalinity bicarbonates (mg.L^{-1})	660.0
Total phosphorus (mg.L^{-1})	8.0
COD (mgO_2.L^{-1})	106.0

* Detection limit of the adopted analysis

2.4. Electrocoagulation

The electrocoagulation unit of 1x1x0.8m^3 was built in polyethylene structure, pointed by Rech [41], for better economic viability, long durability and low cost compared to other materials. Energy expenditures and aluminum plates were obtained experimentally, as mentioned above. In scenario S3, the energy generated by biogas was allocated to the process and the excess was accounted for as output in the system. Data are shown in Table 3.

Table 3. Electrocoagulation unit.

Scenario	Input	Quantity	SimaPro® data
S1, S2, S3	Polyethylene (kg)	2.4948E^{-4}	Polyethylene high density granulates (PE-HD), production mix, at plant RER
S1, S2, S3	Polyethylene molding (kg)	2.4948E^{-4}	Injection molding (CA-QC) injection molding - APOS, S
S1, S2, S3	Aluminum plate (kg)	2.52	Aluminum, cast alloy GLO market for APOS, S
S1, S2	Electricity (kWh)	2.25	Electricity, low voltage (BR- south-eastern grid) market for electricity, low voltage APOS, S
S3	Electricity (kWh)	2.25	Electricity, low voltage (CH) biogas, burned in micro gas turbine 100kWe - APOS, S

Functional unit: 1m^3 of effluent; lifetime 25 years.

2.5. Sedimentation unit

The costs of inputs and energy with the structure and operation of the sedimentation unit were estimated based on the study of Cashman et al. [59], presented in **Table 4**. The sedimentation unit of concrete and steel frame structures supported the polyethylene apparatus and stirring system. For all scenarios, the output of effluent treated to 10mg.L^{-1} of fluoride was considered, including the other parameters shown in **Table 2**, except for COD (Chemical oxygen demand) and aluminum.

Table 4. Sedimentation unit.

	Scenario	Input	Quantity	SimaPro® data
Sedimentation tank	S1, S2, S3	Steel (kg)	8.8E-4	Iron and steel, production mix/US
	S1, S2, S3	HDPE (kg)	5.8E-6	Polyethylene high density granulates (PE-HD), production mix, at plant RER

structure	S1, S2, S3	Concrete (m^3)	1.0E-5	Concrete, normal (BR) market for concrete, normal - APOS, S
Motor	S1, S2, S3	Steel (kg)	2.4E-8	Iron and steel, production mix/US
	S1, S2, S3	Steel (kg)	6.0E-9	Iron and steel, production mix/US
	S1, S2, S3	Cast iron (kg)	1.8E-7	Cast iron (GLO) market for - APOS S
	S1, S2, S3	Aluminum (kg)	5.4E-9	Aluminum alloy, AlLi (GLO) market for - APOS, S
	S1, S2, S3	Cooper (kg)	4.6E-9	Copper sheet, technology mix, consumption mix, at plant, 0.6mm thickness EU-15 S
	S1, S2	Electricity (kWh)	0.092	Electricity, low voltage (BR- south-eastern grid) market for electricity, low voltage APOS, S
	S3	Electricity (kWh)	0.092	Electricity, low voltage (CH) biogas, burned in micro gas turbine 100kWe - APOS, S
Functional unit: 1m³ of effluent; Lifetime of sedimentation tank: 100 years; Motor lifetime: 25 years. APOS (Allocation at the point of substitution)				

2.6. pH adjustment unit

The pH adjustment unit is composed by 200L polyethylene barrel and receives the controlling-pH reagents (Table 5). As mentioned earlier, in scenarios S2 and S3, biogas was injected into the effluent for pH control. According to Nigri et al. [30], only the CO_2 reacts with the effluent reducing the pH. Methane content in biogas increases due to CO_2 removal, which benefits the energy generation process.

Table 5. pH adjustment unit inventory.

Scenario	Input	Output	Quantity	SimaPro® data
S1, S2, S3	Polyethylene (g)		0.044074	Polyethylene high density granulates (PE-HD), production mix, at plant RER
S1, S2, S3	Polyethylene molding (g)		0.044074	Injection molding (CA-QC) injection molding - APOS, S
S1	HCl (L)		2.627	Hydrochloric acid, Mannheim process (30% HCl), at plant/RER Mass
S2, S3	Biogas (L)		5.3966	Biogas, from grass (CH) biogas production from grass – APOS S
S3		Electricity (kwh)	*15.04857	Electricity, low voltage (CH) biogas, burned in micro gas turbine 100kWe - APOS, S
Functional unit: 1m³ of effluent; lifetime: 25 years. *Excess energy in the process				

The consumption of CO_2 of 5.31kg.m^{-3} was obtained by modeling the system using the geochemical software PHREEQC, Version 3.4.0.1 2927 (llnl.dat), for a closed system. Furthermore, the energy capacity of gas after pH control can be increased by the generation of hydrogen in the electrocoagulation process. For scenario S2, the output of methane (1,894kg.m^{-3}) was allocated to the atmosphere, regarding the consumption of CO_2 in the process. Considering that biogas can generate 8.25kWh.m^{-3}as pointed by Dalpaz [60], and a 40% yield due to losses in the collection and in the process of obtaining electricity, the energy generated by the volume of gas spent in the process was 17.81kWh.m^{-3}. In scenario S3 the biogas was converted into electrical energy that was used in the process.

2.7. Pumping unit

The pumping unit (Table 6) is composed of pumps (4 units) and pipelines (30 m). Structural data were estimated based on the study of Cashman et al. [59], and the energy expenditures were based on the study of Singh et al. [57].

Table 6. Pumping unit inventory.

	Scenario	Input	Quantity	SimaPro® data
Pickup pump	S1, S2, S3	Cast iron (kg)	2.4E^{-5}	Cast iron (GLO) market for – APOS, S
	S1, S2, S3	Stainless steel (kg)	2.2E^{-6}	Steel, stainless 304, flat rolled coil/kg/RNA

Preprints.org (www.preprints.org) | NOT PEER-REVIEWED | Posted: 16 September 2025 doi:10.20944/preprints202509.1426.v1

	S1, S2	Electricity (kWh)	0.203	Electricity, low voltage (BR- south-eastern grid) market for electricity, low voltage APOS, S
	S3	Electricity (kWh)	0.203	Electricity, low voltage (CH) biogas, burned in micro gas turbine 100kWe - APOS, S
Acid or biogas injection pump	S1, S2, S3	Cast iron (kg)	$1.3E^{-7}$	Cast iron (GLO) market for – APOS, S
	S1, S2, S3	Stainless steel (kg)	$9.1E^{-8}$	Steel, stainless 304, flat rolled coil/kg/RNA
	S1, S2	Electricity (kWh)	0.0156	Electricity, low voltage (BR- south-eastern grid) market for electricity, low voltage APOS, S
	S3	Electricity (kWh)	0.0156	Electricity, low voltage (CH) biogas, burned in micro gas turbine 100kWe - APOS, S
Sludge pump	S1, S2, S3	Cast iron (kg)	$2.8E^{-7}$	Cast iron (GLO) market for – APOS, S
	S1, S2, S3	Stainless steel (kg)	$1.9E^{-7}$	Steel, stainless 304, flat rolled coil/kg/RNA
	S1, S2	Electricity (kWh)	0.0165	Electricity, low voltage (BR- south-eastern grid) market for electricity, low voltage APOS, S
	S3	Electricity (kWh)	0.0165	Electricity, low voltage (CH) biogas, burned in micro gas turbine 100kWe - APOS, S
Treated effluent pump	S1, S2, S3	Cast iron (kg)	$2.4E^{-5}$	Cast iron (GLO) market for – APOS, S
	S1, S2, S3	Stainless steel (kg)	$2.2E^{-6}$	Steel, stainless 304, flat rolled coil/kg/RNA
	S1, S2	Electricity (kWh)	0.183	Electricity, low voltage (BR- south-eastern grid) market for electricity, low voltage APOS, S
	S3	Electricity (kWh)	0.183	Electricity, low voltage (CH) biogas, burned in micro gas turbine 100kWe - APOS, S
Pipe line	S1, S2, S3	PVC pipeline (m)	$3.0983E^{-5}$	PVC pipe E
Functional unit: 1m³ of effluent; pumps lifetime: 25 years; pipes lifetime: 100 years (30m; 100mm).				

2.8. Transport and use of sludge

The sludge removed from the sedimentation unit is conditioned in an open-air place to reduce its humidity. The sludge was transported 40.5 km from the storage area to the brick factory with a moisture content of 20%. In the adopted project, the sludge replaces 10% of mass compounds used in the production of bricks [45]. Thus, at this stage, the clay that will be replaced by the sludge is considered as an output (Table 7).

Table 7. Transport and use of sludge unit inventory.

Scenario	Input	Output	Quantity	SimaPro® data
S1, S2, S3	Transport (t.km)		0.360045	Transport, truck 10-20t, EURO5, 80%LF, empty return/GLO Mass
S1, S2, S3		Sludge (kg)	7.41	Clay (RoW) market for clay - APOS.U
Functional unit: 1m³ of effluent; distance 40.5km; t.km – tons.km				

2.9. System constraints and uncertainties

This study simplifies the environmental impact assessment by considering selected constraints: installing the electrocoagulation unit, wiring and electrical systems, pumps, sludge removal and transport, disposal from the treatment unit, and used HCl transport. Biogas production impacts were modeled in SimaPro® as Biogas (CH) from grass – APOS, S. Aluminum plate exchange was excluded, and outdoor storage of sludge incurred no energy or moisture loss costs.

The parameters for obtaining an effluent with a fluoride concentration below 10 mg/L, such as cathode consumption and energy expenditure were obtained from laboratory scale and estimated for a full-scale unit, which can cause some degree of variation. The amount of biogas used in the process, and consequently the CO_2 consumed, were estimated by simulation in PHREEQC software. A yield of 40% was considered, including the process of obtaining electricity. However, the actual value depends on the generator used and the efficiency of capturing the gas, which was not carried out in this study. The variation of 7.9-10.3mg.L-1 in fluoride concentration with a pH variation of 6.5-7.1 was considered.

Results and Discussion

3.1. Environmental impacts assessed by scenario

The life cycle environmental impacts of the three scenarios were assessed using the ReCiPe Endpoint Method (E) and are shown in Figure 4. In general, the environmental impact presented in scenario S3 (6,37 Pt) was lower than S1 (12,52 Pt) and S2 (13,09 Pt) mainly due to the use of biogas for pH control and electricity co-generation. Scenario S2 shows the largest environmental impact even with biogas as a pH regulator. This means that exclusive substitution of HCl for biogas was not beneficial, even though this origin from biomass residues. Perhaps, this increment on the impact evaluation comes from the release of methane and carbon dioxide into the environment. Furthermore, the impact on human health was the most significant compared to the impacts generated using natural resources and caused to ecosystems.

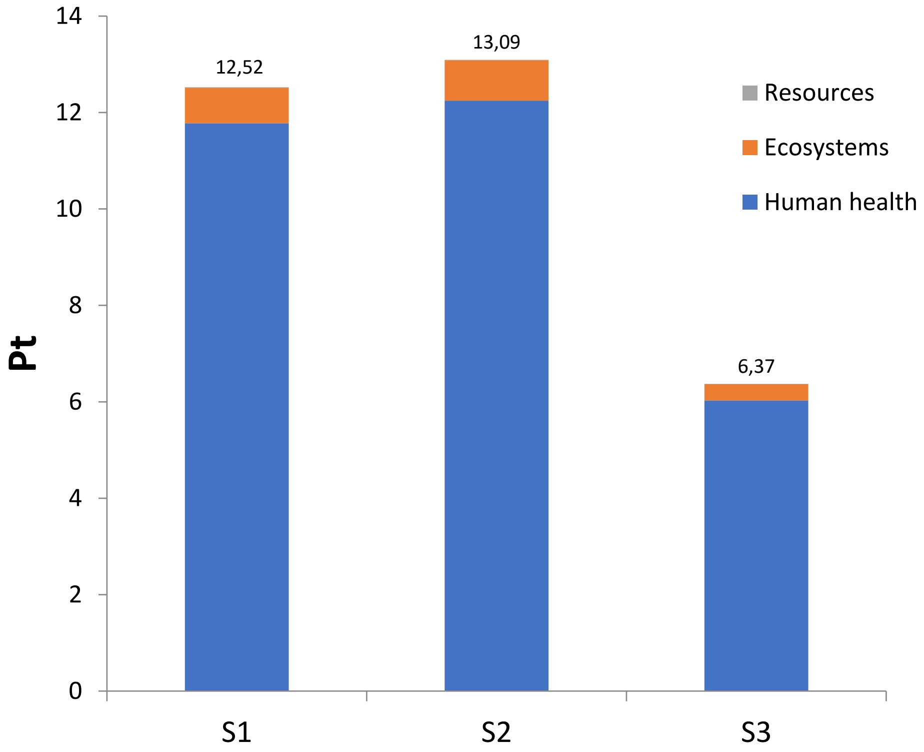

Figure 4. Overall impacts of three water treatment scenarios using ReCiPe endpoint method (E). S1- Scenario 1; S2- Scenario 2; S3- Scenario 3.

In general, the fluoride removal process by electrocoagulation had a negative environmental impact, even though the use of biogas for electric energy co-generation and the use of sludge in the production of bricks. It was observed a reduction in the overall score from 12.5 (S1), commonly used, to 6.4 (S3), when biogas was used, i.e., 50% lower environmental impact. The use of sludge in brick production was constant across all scenarios, so further consideration of this factor was unnecessary.

The individual impacts across 22 categories (in percentages) were assessed with the ReCiPe midpoint method, as shown in Figure 5. Scenario S3 had the lowest overall environmental impact but showed a drawback in stratospheric ozone depletion. Its primary benefit is converting biogas into electrical energy for process use, with additional surplus generation.

Figure 6 compares environmental impacts by category and normalized score. The main impacts from fluoride removal were human non-carcinogenic and carcinogenic toxicity, global warming, human health, marine ecotoxicity, and fine particulate formation. Scenario 3 had the lowest environmental impact.

Preprints.org (www.preprints.org) | NOT PEER-REVIEWED | Posted: 16 September 2025 doi:10.20944/preprints202509.1426.v1

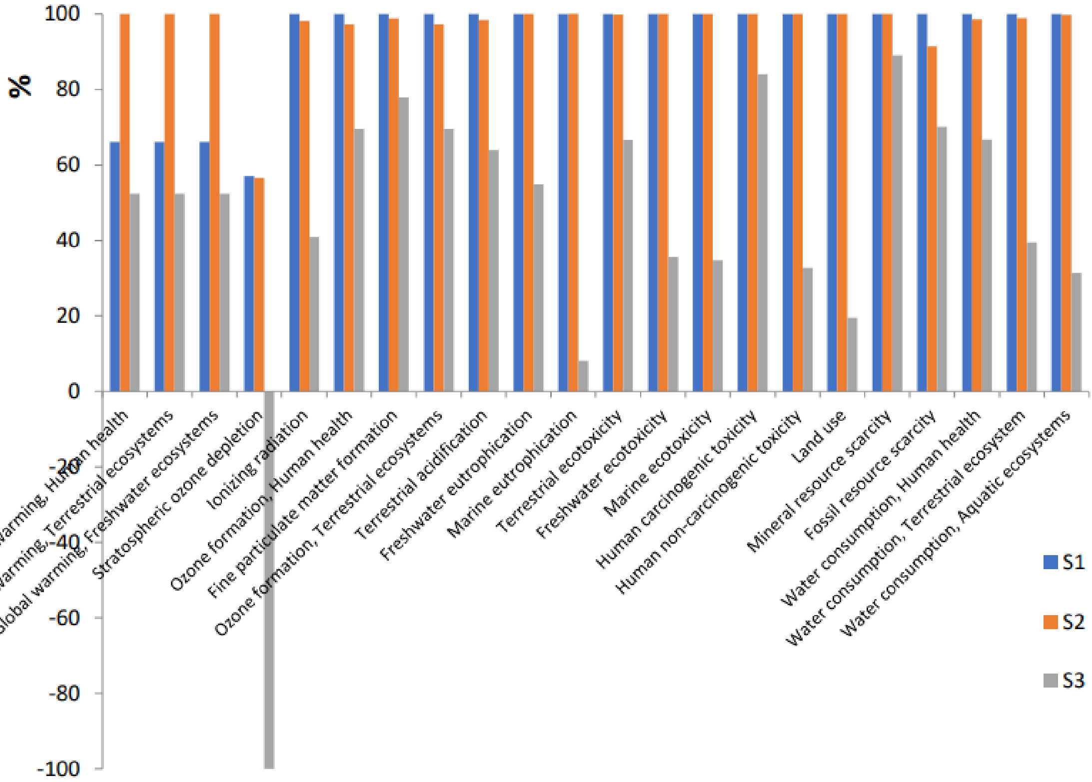

Figure 5. Percentage-based normalized environmental impacts for 22 categories, generated from three scenarios using the ReCiPe endpoint method. S1 refers to Scenario 1; S2 to Scenario 2; S3 to Scenario 3.

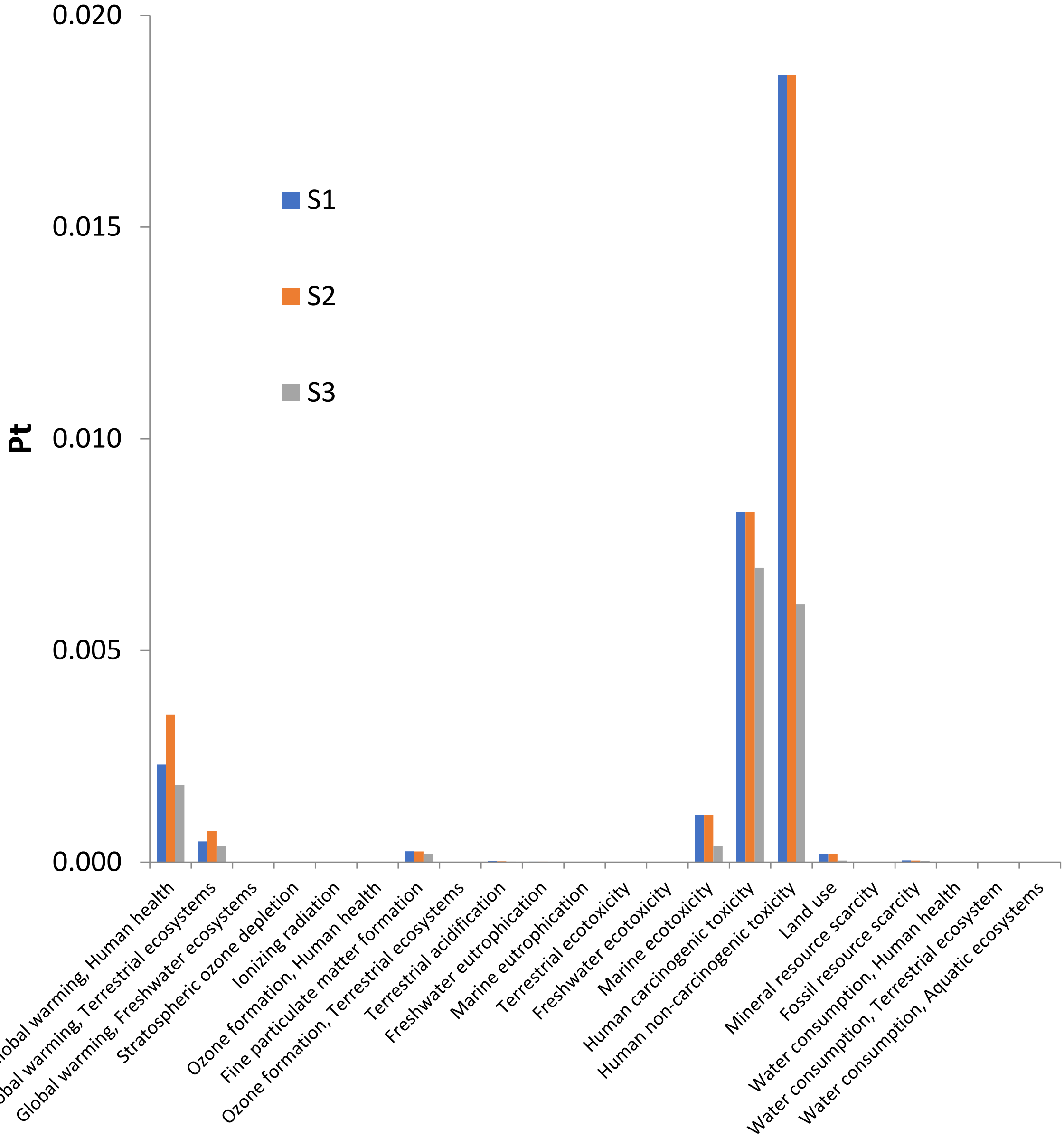

Figure 6. Individual environmental impacts normalized of 22 categories generated from three scenarios using ReCiPe endpoint method. S1- Scenario 1; S2- Scenario 2; S3- Scenario 3.

Among the subsystems evaluated (electrocoagulation unit, pH adjustment unit, sedimentation unit, pumping unit, and sludge transport unit), the electrocoagulation unit exhibits the greatest environmental impact. Conversely, in scenario S3 (Figure 7), the pH adjustment unit demonstrates a net negative impact, attributed to electricity generation from biogas.

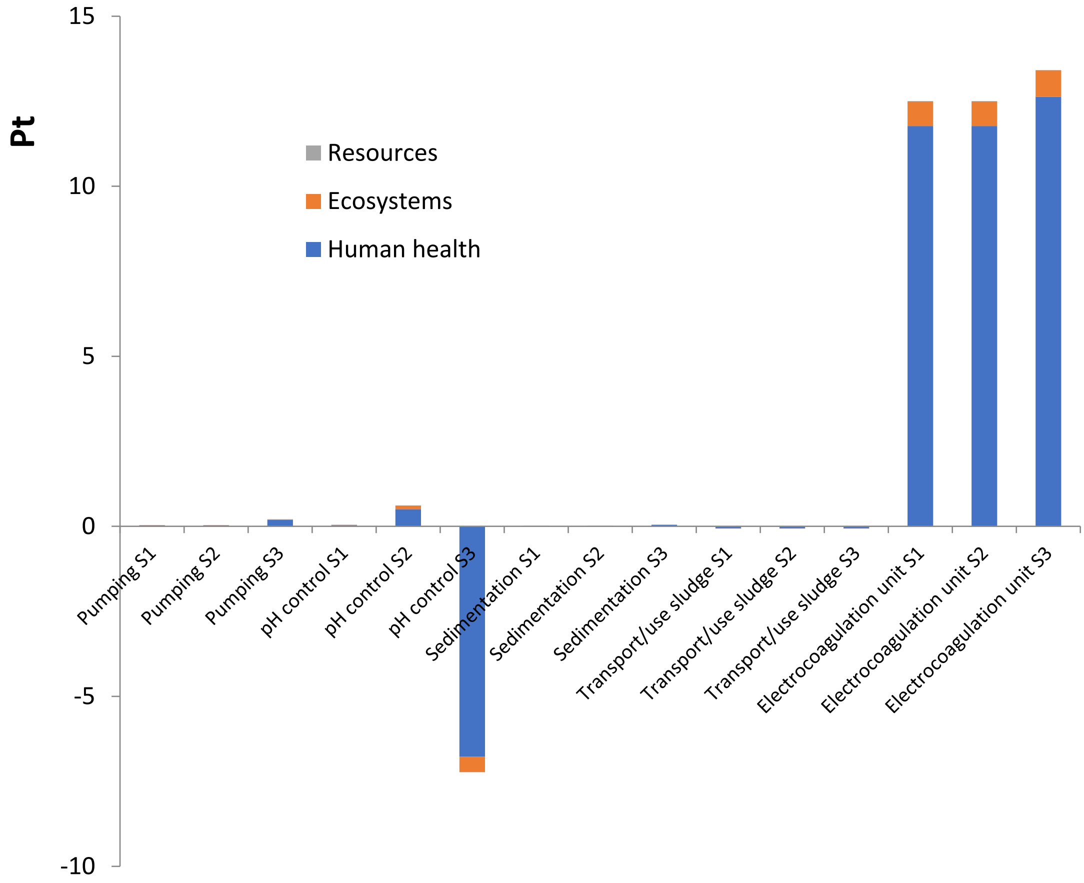

Figure 7. Overall impacts of subsystems units from three water treatment scenarios using ReCiPe endpoint method (E), S1- Scenario 1; S2- Scenario 2; S3- Scenario 3.

3.2. Environmental impacts by subsystems

Figure 8 shows the individual impacts. Scenario S3 has the greatest environmental impact, likely because of differences in electrical energy sources. Since Brazil's energy mainly comes from hydroelectric power, its impact is lower than biogas, which emits CO_2 directly.

In the analysis of the pumping and sedimentation subsystems (Figure 9), the processes differ only in their sources of electrical energy. Electricity derives from biogas combustion, which releases CO_2 and other gases associated with human non-carcinogenic and carcinogenic toxicity as well as terrestrial ecotoxicity. These effects are reduced when electricity is produced by a hydroelectric power plant.

Figure 10 illustrates the adverse environmental impacts associated with employing biogas for electricity generation and pH adjustment subsystems. This outcome is attributed to the excess electricity produced in scenario S3. It should be noted that employing biogas exclusively for pH adjustment results in a higher environmental impact (S2) compared to conducting pH adjustment with acid (S1). In the sludge transport and utilization subsystem (Figure 11), a negative environmental effect has been identified when electrocoagulation waste is used as an input for brick production [45]. Additionally, there were no significant differences observed among these scenarios; the environmental impacts remained consistent across S1, S2, and S3 within the scope of this study.

Preprints.org (www.preprints.org) | NOT PEER-REVIEWED | Posted: 16 September 2025 doi:10.20944/preprints202509.1426.v1

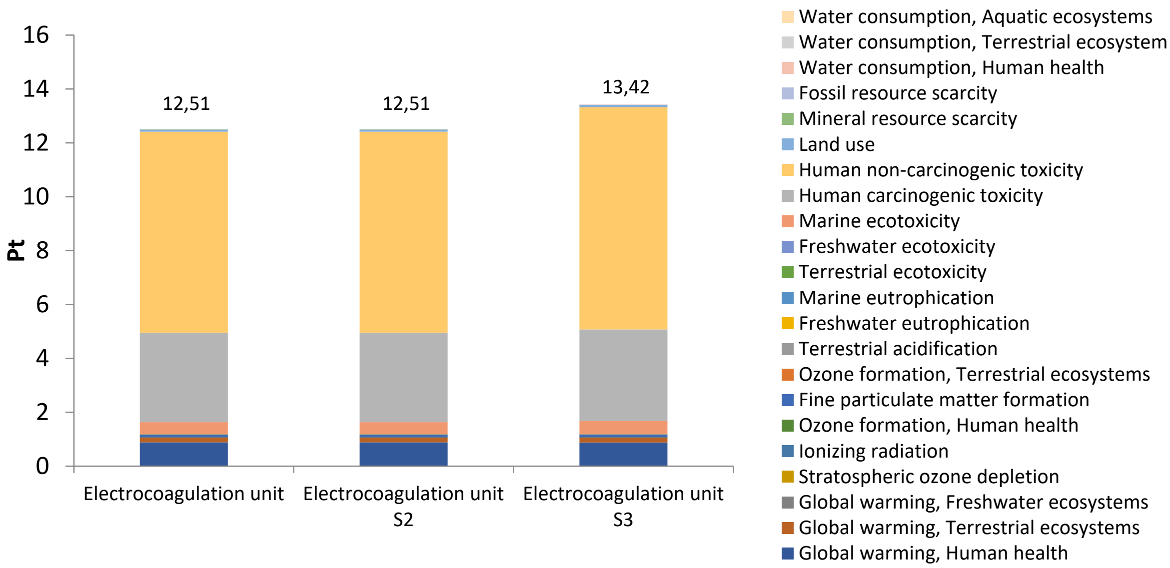

Figure 8. Environmental impacts from electrocoagulation subsystem with ReCiPe endpoint method (E), S1- Scenario 1; S2- Scenario 2; S3- Scenario 3.

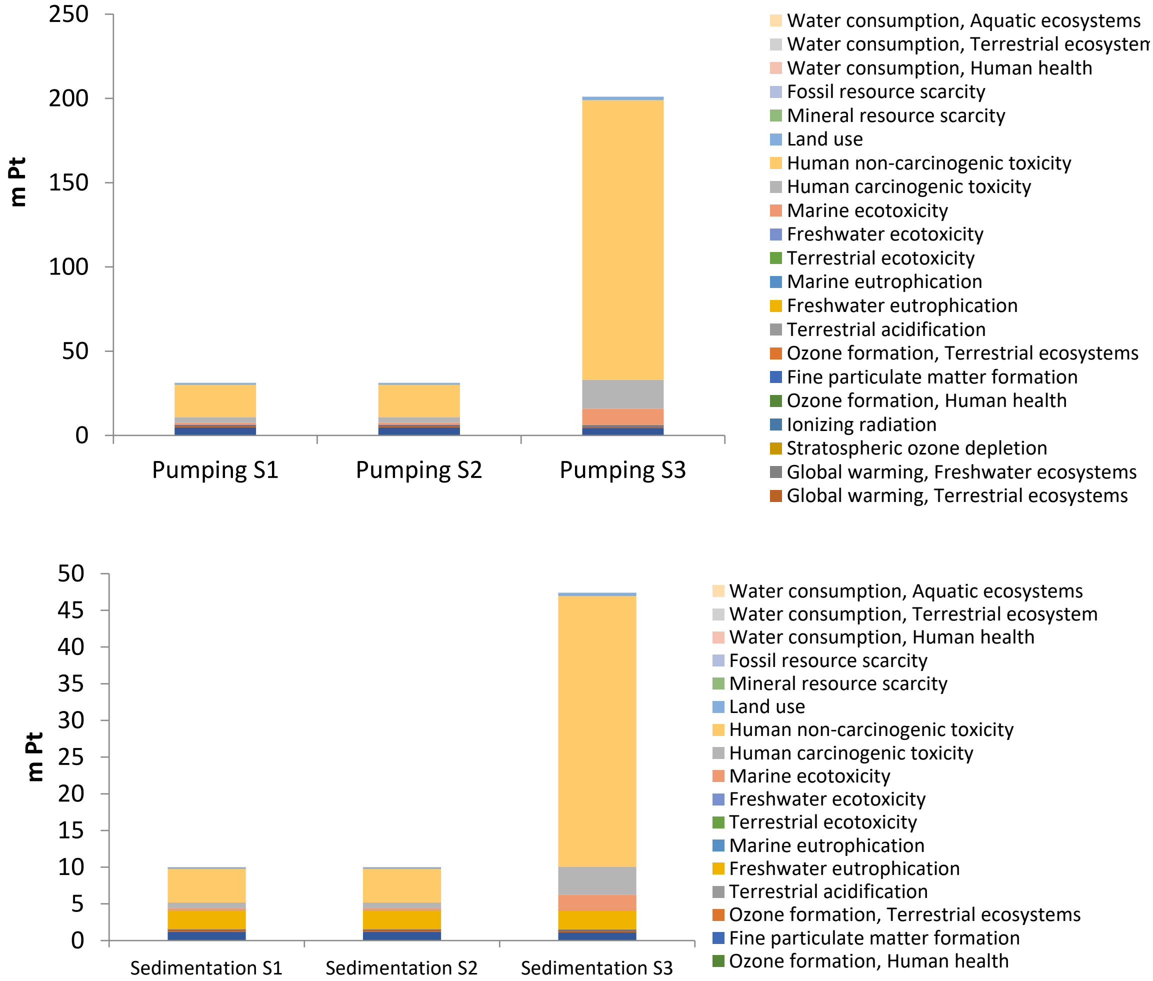

Figure 9. Environmental impacts from pumping and sedimentation subsystems with ReCiPe endpoint method (E), S1- Scenario 1; S2- Scenario 2; S3- Scenario 3.

Preprints.org (www.preprints.org) | NOT PEER-REVIEWED | Posted: 16 September 2025 doi:10.20944/preprints202509.1426.v1

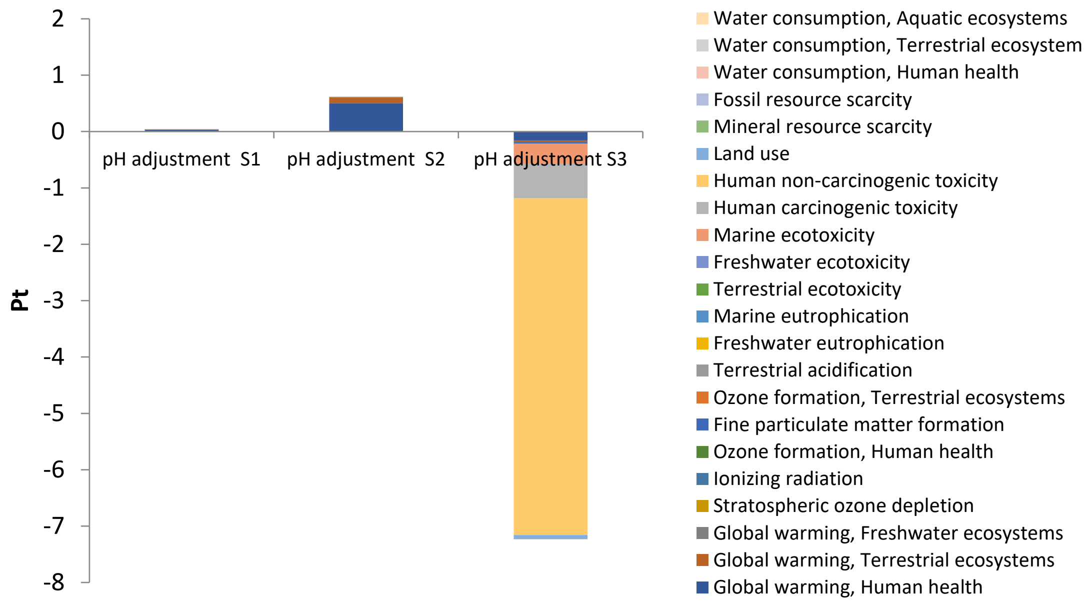

Figure 10. Environmental impacts from pH adjustment subsystem with ReCiPe endpoint method (E), S1- Scenario 1; S2- Scenario 2; S3- Scenario 3.

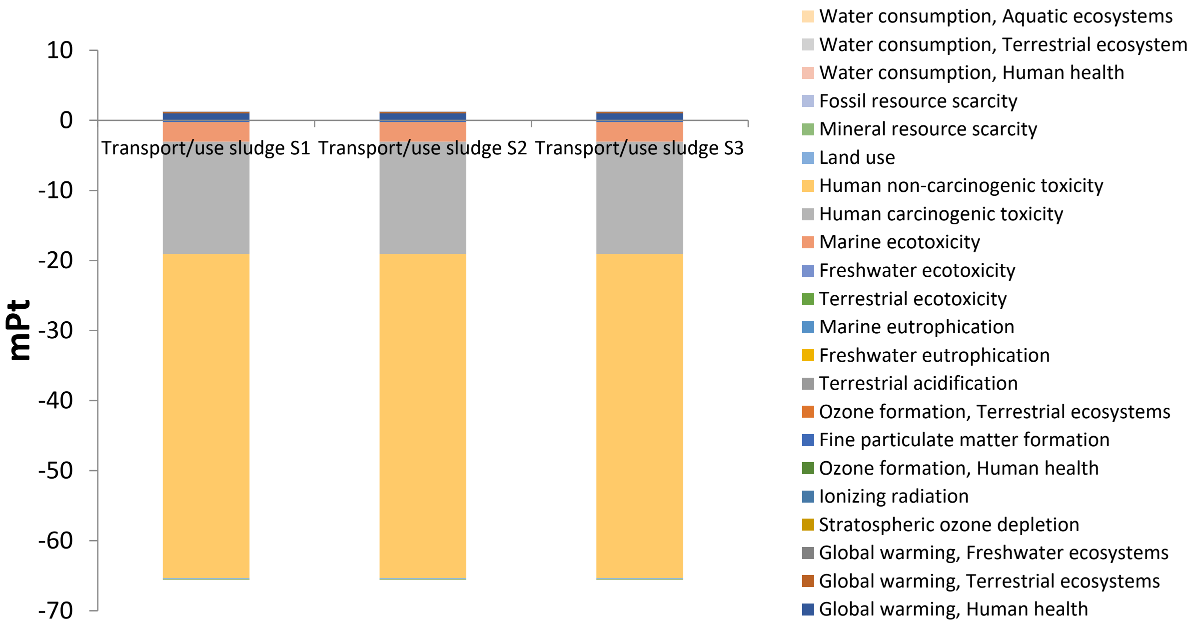

Figure 11. Environmental impacts from sludge transport subsystem and its use as an input in brick production with ReCiPe endpoint method (E), S1- Scenario 1; S2- Scenario 2; S3- Scenario 3.

4. Conclusions

Using biogas-derived CO_2 for cogeneration reduced environmental impacts from 12.52 Pt (S2) to 6.37 Pt (S3). In contrast, using biogas solely for pH adjustment (S2) increased impacts compared with traditional hydrochloric acid (S1). The main contributions, particularly toxicity, global warming potential, marine ecotoxicity, and particulate matter formation were associated with the electrocoagulation subsystem. Although S3 showed slightly higher impacts in these categories due to biogas combustion, this was offset by the energy gains and sludge reuse. Overall, the results indicate that biogas utilization provides environmental benefits primarily when applied to cogeneration, rather than as a substitute for HCl. Among all impact categories, effects on human health were the most pronounced.

Acknowledgements: The authors acknowledge the Brazilian research funding agencies CAPES for the postdoctoral scholarship, CNPq (Process 308044/2018-5), and FAPEMIG for financial support. The authors also thank SimaPro® for providing the academic free license.

References

1. Santhi, V.M.; Periasamy, D.; Perumal, M.; Sekar, P.M.; Varatharajan, V.; Aravind, D.; Senthilkumar, K.; Kumaran, S.T.; Ali, S.; Sankar, S.; Vijayakumar, N.; Boominathan, C.; Krishnan, R.S. The global challenge of fluoride contamination: A comprehensive review of removal processes and implications for human health and ecosystems. *Sustainability* **2024**, *16*, 11056. https://doi.org/10.3390/su162411056
2. Ahmad, S.; Singh, R.; Arfin, T.; Neeti, K. Fluoride contamination, consequences and removal techniques in water: A review. *Environmental Science: Advances* **2022**, *1*, 620–661. https://doi.org/10.1039/d1va00039j
3. Reardon, E.J.; Wang, Y. A limestone reactor for fluoride removal from wastewaters. *Environmental Science & Technology* **2000**, *34*, 3247–3253. https://doi.org/10.1021/es990542k
4. de Luna, M.D.G.; Warmadewanthi; Liu, J.C. Combined treatment of polishing wastewater and fluoride-containing wastewater from a semiconductor manufacturer. *Colloids and Surfaces A: Physicochemical and Engineering Aspects* **2009**, *347*, 64–68. https://doi.org/10.1016/j.colsurfa.2008.12.006
5. Chiu, T.C.; Huang, H.-C.; Chen, L.J. Treatment of semiconductor wastewater by dissolved air flotation. *Journal of Environmental Engineering* **2002**, *128*, 974–980. https://doi.org/10.1061/(ASCE)0733-9372(2002)128:10(974)
6. Drouiche, N.; Ghaffour, N.; Aoudj, S.; Hecini, M.; Ouslimane, T. Fluoride removal from photovoltaic wastewater by aluminium electrocoagulation and characteristics of products. *Chemical Engineering Transactions* **2009**, *17*, 1651–1656. https://doi.org/10.3303/CET0917276
7. Ezzeddine, A.; Bedoui, A.; Hannachi, A.; Bensalah, N. Removal of fluoride from aluminum fluoride manufacturing wastewater by precipitation and adsorption processes. *Desalination and Water Treatment* **2015**, *54*, 2280–2292. https://doi.org/10.1080/19443994.2014.899515
8. Khatibikamal, V.; Torabian, A.; Janpoor, F.; Hoshyaripour, G. Fluoride removal from industrial wastewater using electrocoagulation and its adsorption kinetics. *Journal of Hazardous Materials* **2010**, *179*, 276–280. https://doi.org/10.1016/j.jhazmat.2010.02.089
9. Toyoda, A.; Taira, T. A new method for treating fluorine wastewater to reduce sludge and running costs. *IEEE Transactions on Semiconductor Manufacturing* **2000**, *13*, 305–309. https://doi.org/10.1109/66.857940
10. Harrison, P.T.C. Fluoride in water: A UK perspective. *Journal of Fluorine Chemistry* **2005**, *126*, 1448–1456. https://doi.org/10.1016/j.jfluchem.2005.09.009
11. Tripathy, S.S.; Bersillon, J.-L.; Gopal, K. Removal of fluoride from drinking water by adsorption onto alum impregnated activated alumina. *Separation and Purification Technology* **2006**, *50*, 310–317. https://doi.org/10.1016/j.seppur.2005.11.036
12. Xiong, X.; Liu, J.; He, W.; Xia, T.; He, P.; Chen, X.; Yang, K.; Wang, A. Dose–effect relationship between drinking water fluoride levels and damage to liver and kidney functions in children. *Environmental Research* **2007**, *103*, 112–116. https://doi.org/10.1016/j.envres.2006.05.008
13. Sharma, P.; Verma, P.K.; Sood, S.; Singh, M.; Verma, D. Impact of chronic sodium fluoride toxicity on antioxidant capacity, biochemical parameters, and histomorphology in cardiac, hepatic, and renal tissues of Wistar rats. *Biological Trace Element Research* **2022**, *200*, 229–241. https://doi.org/10.1007/s12011-022-03113-w
14. Sun, Y.; Zhang, C.; Ma, J.; Sun, W.; Shah, K.J. Review of fluoride removal technology from wastewater environment. *Desalination and Water Treatment* **2023**, *299*, 90–101. https://doi.org/10.5004/dwt.2023.29668
15. Mameri, N.; Yeddou, A.R.; Lounici, H.; Belhocine, D.; Grib, H.; Bariou, B. Defluoridation of septentrional Sahara water of North Africa by electrocoagulation process using bipolar aluminium electrodes. *Water Research* **1998**, *32*, 1604–1612. https://doi.org/10.1016/S0043-1354(97)00357-6

16. Guzmán, A.; Nava, J.L.; Coreño, O.; Rodríguez, I.; Gutiérrez, S. Arsenic and fluoride removal from groundwater by electrocoagulation using a continuous filter press reactor. *Chemosphere* **2016**, *144*, 2113–2120. https://doi.org/10.1016/j.chemosphere.2015.10.108
17. Drondina, R.V.; Drako, I.V. Electrochemical technology of fluorine removal from underground and waste waters. *Journal of Hazardous Materials* **1994**, *37*, 91–100. https://doi.org/10.1016/0304-3894(94)85037-2
18. Yang, C.-L.; Dluhy, R. Electrochemical generation of aluminum sorbent for fluoride adsorption. *Journal of Hazardous Materials* **2002**, *94*, 239–252. https://doi.org/10.1016/S0304-3894(02)00066-3
19. Shen, F.; Chen, X.; Gao, P.; Chen, G. Electrochemical removal of fluoride ions from industrial wastewater. *Chemical Engineering Science* **2003**, *58*, 987–993. https://doi.org/10.1016/S0009-2509(02)00639-5
20. Emamjomeh, M.M.; Sivakumar, M. An empirical model for defluoridation by batch monopolar electrocoagulation/flotation (ECF) process. *Journal of Hazardous Materials* **2006**, *131*, 118–125. https://doi.org/10.1016/j.jhazmat.2005.09.030
21. Zhu, J.; Zhao, H.; Ni, J. Fluoride distribution in electrocoagulation defluoridation process. *Separation and Purification Technology* **2007**, *56*, 184–191. https://doi.org/10.1016/j.seppur.2007.01.030
22. Tezcan Un, U.; Koparal, A.S.; Ogutveren, U.B. Fluoride removal from water and wastewater with a batch cylindrical electrode using electrocoagulation. *Chemical Engineering Journal* **2013**, *223*, 110–115. https://doi.org/10.1016/j.cej.2013.02.126
23. Sandoval, M.A.; Fuentes, R.; Nava, J.L.; Rodríguez, I. Fluoride removal from drinking water by electrocoagulation in a continuous filter press reactor coupled to a flocculator and clarifier. *Separation and Purification Technology* **2014**, *134*, 163–170. https://doi.org/10.1016/j.seppur.2014.07.034
24. Yetilmezsoy, K.; Dehghani, M.H.; Saeedi, R.; Dalvand, A.; Heibati, B.; Askari, M.; Alimohammadi, M.; McKay, G. Elimination of natural organic matter by electrocoagulation using bipolar and monopolar arrangements of iron and aluminum electrodes. *International Journal of Environmental Science and Technology* **2017**, *14*, 2125–2134. https://doi.org/10.1007/s13762-017-1402-3
25. Garg, U.K.; Sharma, C.; Garg, U.K. Electrocoagulation: Promising technology for removal of fluoride from drinking water—A review. *Biological Forum* **2016**, *8*, 248–254. Available online: http://www.researchtrend.net (accessed on 18 March 2019).
26. Nigri, E.; Santos, A.; Rocha, S. Electrocoagulation associated with CO_2 mineralization applied to fluoride removal from mining industry wastewater. *Desalination and Water Treatment* **2021**, *209*, 58–70. https://doi.org/10.5004/dwt.2021.26520
27. Astuti, A.R.A.; Mutiara, S.; Saputera, N. Advances in carbon control technologies for flue gas: A step towards sustainable industrial CO_2 capture. *International Journal of Greenhouse Gas Control* **2024**, *123*, 103587. https://doi.org/10.1080/15422119.2024.2328080
28. Beiron, J.; Normann, F.; Kristoferson, L.; Strömberg, L.; Gardarsdóttir, S.Ö.; Johnsson, F. Enhancement of CO_2 absorption in water through pH control and carbonic anhydrase—A technical assessment. *Industrial & Engineering Chemistry Research* **2019**, *58*, 14275–14283. https://doi.org/10.1021/acs.iecr.9b02688
29. Werkneh, A.A. Biogas impurities: Environmental and health implications, removal technologies and future perspectives. *Heliyon* **2022**, *8*, e10929. https://doi.org/10.1016/j.heliyon.2022.e10929
30. Ahangarnokolaei, R.; Rahmanian, N.; Ramezani, M.; Khataee, A. Environmental performance of electrocoagulation and ozonation for wastewater treatment: A life cycle assessment approach. *Journal of Environmental Management* **2021**, *287*, 112345. https://doi.org/10.1016/j.jenvman.2021.112345
31. Choudhary, N.; Singh, P.; Kumar, R.; Gupta, S. Life cycle assessment of electrocoagulation processes: Energy consumption and global warming potential. *Journal of Cleaner Production* **2023**, *408*, 137137. https://doi.org/10.1016/j.jclepro.2023.137137
32. Li, Y.; Zhang, H.; Chen, Q.; Wang, J. Performance of aluminum electrodes in electrocoagulation for removal of heavy metals and phosphorus. *Chemosphere* **2024**, *351*, 139876. https://doi.org/10.1016/j.chemosphere.2023.139876
33. Zailani, S.; Zin, R.M. Electrocoagulation for wastewater treatment: Influence of electrode material and process parameters. *Environmental Technology & Innovation* **2018**, *10*, 123–131. https://doi.org/10.1016/j.eti.2018.01.009

34. Li, Y.; Zhang, S.; Zhang, W.; Xiong, W.; Ye, Q.; Hou, X.; Wang, C.; Wang, P. Life cycle assessment of advanced wastewater treatment processes: Involving 126 pharmaceuticals and personal care products in life cycle inventory. *Journal of Environmental Management* **2019**, *238*, 442–450. https://doi.org/10.1016/j.jenvman.2019.01.118
35. ISO. ISO 14040:2006. Environmental Management—Life Cycle Assessment—Principles and Framework, 2nd ed.; International Organization for Standardization: Geneva, Switzerland, 2006. Available online: https://www.iso.org/standard/37456.html (accessed on 15 September 2025).
36. Pell, R.; Tijsseling, L.; Palmer, L.W.; Glass, H.J.; Yan, X.; Wall, F.; Zeng, X.; Li, J. Environmental optimisation of mine scheduling through life cycle assessment integration. *Resources, Conservation and Recycling* **2019**, *142*, 267–276. https://doi.org/10.1016/j.resconrec.2018.11.022
37. Rahman, S.M.; Eckelman, M.J.; Onnis Hayden, A.; Gu, A.Z. Comparative life cycle assessment of advanced wastewater treatment processes for removal of chemicals of emerging concern. *Environmental Science & Technology* **2018**, *52*, 11346–11358. https://doi.org/10.1021/acs.est.8b00036
38. Opher, T.; Friedler, E. Comparative LCA of decentralized wastewater treatment alternatives for non-potable urban reuse. *Journal of Environmental Management* **2016**, *182*, 464–476. https://doi.org/10.1016/j.jenvman.2016.07.080
39. Castellet, L.; Molinos-Senante, M. Efficiency assessment of wastewater treatment plants: A data envelopment analysis approach integrating technical, economic, and environmental issues. *Journal of Environmental Management* **2016**, *167*, 160–166. https://doi.org/10.1016/j.jenvman.2015.11.037
40. Corominas, L.; Foley, J.; Guest, J.S.; Hospido, A.; Larsen, H.F.; Morera, S.; Shaw, A. Life cycle assessment applied to wastewater treatment: State of the art. *Water Research* **2013**, *47*, 5480–5492. https://doi.org/10.1016/j.watres.2013.06.049
41. Goyal, H.; Mondal, P. Life cycle assessment (LCA) of the arsenic and fluoride removal from groundwater through adsorption and electrocoagulation: A comparative study. *Chemosphere* **2022**, *304*, 135243. https://doi.org/10.1016/j.chemosphere.2022.135243
42. Thakur, L.S.; Goyal, H.; Mondal, P. Simultaneous removal of arsenic and fluoride from synthetic solution through continuous electrocoagulation: Operating cost and sludge utilization. *Journal of Environmental Chemical Engineering* **2019**, *7*, 102829. https://doi.org/10.1016/j.jece.2018.102829
43. Çetinkaya, A.Y. Integration of electrocoagulation and solar energy for sustainable wastewater treatment: A thermodynamic and life cycle assessment study. *Environmental Monitoring and Assessment* **2025**, *197*, 224. https://doi.org/10.1007/s10661-025-13662-x
44. Sharma, P.; Joshi, H. Utilization of electrocoagulation treated spent wash sludge in making building blocks. *International Journal of Environmental Science and Technology* **2016**, *13*, 349–358. https://doi.org/10.1007/s13762-015-0845-7
45. Rajaniemi, K.; Tuomikoski, S.; Lassi, U. Electrocoagulation sludge valorization—A review. *Resources* **2021**, *10*, 127. https://doi.org/10.3390/resources10120127
46. Zhu, P.; Li, J.; Wang, L.; Zhou, R.; Liu, Y. Reuse of hazardous calcium fluoride sludge in ceramic products. *Journal of Hazardous Materials* **2013**, *260*, 855–860. https://doi.org/10.1016/j.jhazmat.2013.06.047
47. Yilmaz, A.E.; Boncukcuoğlu, R.; Kocakerim, M.; Karakaş, İ.H. Waste utilization: The removal of textile dye (Bomaplex Red CR L) from aqueous solution on sludge waste from electrocoagulation as adsorbent. *Desalination* **2011**, *277*, 156–163. https://doi.org/10.1016/j.desal.2011.04.018
48. García Gómez, C.; Rivera Huerta, M.L.; Almazán García, F.; Martín Domínguez, A.; Romero Soto, I.C.; Burboa Charis, V.A.; Gortáres Moroyoqui, P. Electrocoagulated metal hydroxide sludge for fluoride and arsenic removal in aqueous solution: Characterization, kinetic, and equilibrium studies. *Water, Air, & Soil Pollution* **2016**, *227*, 96. https://doi.org/10.1007/s11270-016-2783-5
49. Golder, A.K.; Samanta, A.N.; Ray, S. Removal of phosphate from aqueous solutions using calcined metal hydroxides sludge waste generated from electrocoagulation. *Separation and Purification Technology* **2006**, *52*, 102–109. https://doi.org/10.1016/j.seppur.2006.03.027
50. Santana, J.J.; Mena, V.F.; Betancor Abreu, A.; Rodríguez Raposo, R.; Izquierdo, J.; Souto, R.M. Use of alumina sludge arising from an electrocoagulation process as functional mesoporous microcapsules for

active corrosion protection of aluminum. *Progress in Organic Coatings* **2021**, *151*, 106044. https://doi.org/10.1016/j.porgcoat.2020.106044

51. ISO. ISO 14044:2006. Environmental Management—Life Cycle Assessment—Requirements and Guidelines, 1st ed.; International Organization for Standardization: Geneva, Switzerland, 2006. Available online: https://www.iso.org/standard/38498.html (accessed on 15 September 2025).
52. Bonton, A.; Bouchard, C.; Barbeau, B.; Jedrzejak, S. Comparative life cycle assessment of water treatment plants. *Desalination* **2012**, *284*, 42–54. https://doi.org/10.1016/j.desal.2011.08.035
53. Goedkoop, M.; Heijungs, R.; Huijbregts, M.; de Schryver, A.; Struijs, J.; van Zelm, R. *ReCiPe 2008: A Life Cycle Impact Assessment Method Which Comprises Harmonised Category Indicators at the Midpoint and the Endpoint Level*; Report I: Characterisation; Ministry of Housing, Spatial Planning and the Environment (VROM): The Hague, The Netherlands, 2009. Available online: https://www.rivm.nl/en/life-cycle-assessment-lca/recipe (accessed on 15 September 2025).
54. Zepon Tarpani, R.R.; Azapagic, A. Life cycle environmental impacts of advanced wastewater treatment techniques for removal of pharmaceuticals and personal care products (PPCPs). *Journal of Environmental Management* **2018**, *215*, 258–272. https://doi.org/10.1016/j.jenvman.2018.03.047
55. Nakhate, P.H.; Moradiya, K.K.; Patil, H.G.; Marathe, K.V.; Yadav, G.D. Case study on sustainability of textile wastewater treatment plant based on life cycle assessment approach. *Journal of Cleaner Production* **2020**, *245*, 118929. https://doi.org/10.1016/j.jclepro.2019.118929
56. Hauschild, M.; Rosenbaum, R.K.; Olsen, S.I. *Life Cycle Assessment: Theory and Practice*; Springer: Cham, Switzerland, 2018. https://doi.org/10.1007/978-3-319-56475-3
57. Singh, P.; Carliell-Marquet, C.; Kansal, A. Energy pattern analysis of a wastewater treatment plant. *Applied Water Science* **2012**, *2*, 221–226. https://doi.org/10.1007/s13201-012-0040-7
58. CONAMA. Resolução 430 (2011). Available online: http://www.suape.pe.gov.br/images/publicacoes/CONAMA_n.430.2011.pdf (accessed on 15 September 2025).
59. Cashman, S.; Gaglione, A.; Mosley, J.; Weiss, L.; Hawkins, T.; Ashbolt, N.; Cashdollar, J.; Xue, X.; Ma, C.; Arden, S. Environmental and cost life cycle assessment of disinfection options for municipal drinking water treatment. *Report*; U.S. Environmental Protection Agency, Office of Research and Development: Cincinnati, OH, USA, 2014. Available online: https://cfpub.epa.gov/si/si_public_record_report.cfm?dirEntryId=298570 (accessed on 15 September 2025).
60. Dalpaz, R. *Avaliação energética do biogás com diferentes percentuais de metano na produção de energia térmica e elétrica*; Master's Thesis, Universidade do Vale do Taquari—Univates, Lajeado, Brazil, 2019. Available online: http://bdtd.ibict.br/vufind/Record/UVAT_1ab6a3b372faa4d5ed630f6c2515c049 (accessed on 15 September 2025).